

ac transport studies of La-modified antiferroelectric lead zirconate thin films

S. S. N. Bharadwaja,* P. Victor, P. Venkateswarulu, and S. B. Krupanidhi†

Materials Research Center, Indian Institute of Science, Bangalore-560 012, India

(Received 7 June 2001; revised manuscript received 14 August 2001; published 23 April 2002)

In recent times antiferroelectric thin-film material compositions have been identified as one of the most significant thin films for development of devices such as high charge storage, charge couplers/decouplers, and high strain microelectromechanical systems. Thus, understanding the dielectric and electrical properties under an ac signal drive in these antiferroelectric thin-film compositions, such as lead zirconate thin films, and the effect of donor doping on them is very necessary. For this purpose, thin films of antiferroelectric lead zirconate and La-modified lead zirconate thin films with mole % concentrations of 0, 3, 5, and 9 have been deposited by pulsed excimer laser ablation. The dielectric and hysteresis properties have confirmed that with a gradual increase of the La content, the room-temperature antiferroelectric lead zirconate thin films can be modified into ferroelectric and paraelectric phases. ac electrical studies revealed that the polaronic related hopping conduction is responsible for the charge transport phenomenon in these films. With a La content of ≤ 3 mole % in pure lead zirconate, the conductivity of the films has been reduced and followed by an increase of its conductivity for a $\geq 3\%$ addition of La to lead zirconate thin films. The polaronic activation energies are also found to follow a similar trend as that of the conductivity.

DOI: 10.1103/PhysRevB.65.174106

PACS number(s): 77.80.-e

I. INTRODUCTION

Ferroelectric Pb-based perovskite oxides such as Pb ($\text{Zr}_{1-x}\text{Ti}_x$) O_3 (PZT) exhibit large varieties of structural and dielectric properties. Ferroelectric solid solutions are of great technological importance for a variety of applications such as memory devices,¹ infrared detectors,² microelectromechanical systems,^{3,4} and electro-optical devices.⁵ Most of the applications are based on spontaneous polarization switching of the ferroelectric medium by an electric field. On the other hand, the end member of the PZT solid solution is PbZrO_3 (PZ), which is a room-temperature antiferroelectric composition and has an orthogonal crystal structure.⁶ Electric-field-induced phase switching between ferroelectric and antiferroelectric phases makes this particular class of thin-film compositions very attractive for the development of high charge storage devices^{7,8} and microelectromechanical systems.^{9,10} From a technological point of view, understanding the transport properties in pure and modified antiferroelectric thin-film compositions will endeavor to convey their physical significance in a concise way. Modification of localized states in microscopic levels reflects in various macroscopic properties of solids, such as electric and optical properties. Consequently, one of the most important problems in the dielectric thin films is to find the relation between the microscopic nature of the charge transport phenomenon and the macroscopic properties of solids. Thus, understanding the high-sensitivity properties such as polarization, dielectric relaxation, and charge transport mechanisms in these oxide thin films can lead to the optimization of functional properties through the appropriate choice of materials.

For microelectronic device applications, various dopants have been used in highlighting specific properties. As a result of doping, the electrical properties change drastically along with the lattice structure of the host material. It has been shown that donor dopings such as La^{3+} and Nb^{5+} with Pb-based oxide thin films have a significant effect on properties

such as polarization switching,¹¹ charge-carrier mobility,¹² and breakdown strength.¹³⁻¹⁵ The interests of a large number of research groups have centered on thin films of ferroelectric PZT solid solutions. Tan *et al.* investigated comprehensively the effect of La^{3+} and K^+ on domain structure and subsequent hysteresis properties in ferroelectric PZT systems.¹⁶ Klissurka *et al.* investigated the effect of Nb_2O_5 on dielectric and switching properties in PZT thin-film system.¹⁷ It has been proposed that in sol-gel and laser ablated PZT thin films, with the greatest uncertainty, polaronic-hopping conductivity is responsible for charge transportation.¹⁸ However, because of the small number of reports on ac conductivity phenomena studied in Pb-based ferroelectric thin films, so far, the nature of the polaronic conductivity mechanisms remained unclear. Earlier attempts have been made to explain transport phenomena in perovskite BaTiO_3 ceramic from the polaronic point of view.¹⁹

In addition to the studies on ferroelectric thin films, there is a need for the parallel growth of research into the electrical properties of antiferroelectric (AFE) thin films. At the present time, a large collection of reliable experimental data of the processing of these AFE thin films has been made available by many research groups.²⁰⁻²⁴ The results of present investigations have shown that the incorporation of dopant can have a remarkable beneficial effect in controlling the dielectric and electrical properties in antiferroelectric PZ thin films.

II. EXPERIMENTAL DETAILS

Ceramic targets of pure and La-modified lead zirconate (PLZ) were prepared via a conventional solid-state synthesis method. Dense ceramic targets of 0, 3, 5, and 9 mole % (denoted as PLZ-0, PLZ-3, PLZ-5, and PLZ-9, respectively) were prepared according to the chemical formula $\text{Pb}_{1-1.5x}\text{La}_x\text{ZrO}_3$. An excess of 10% PbO was taken in the ceramic target in order to avoid volatilization of PbO during

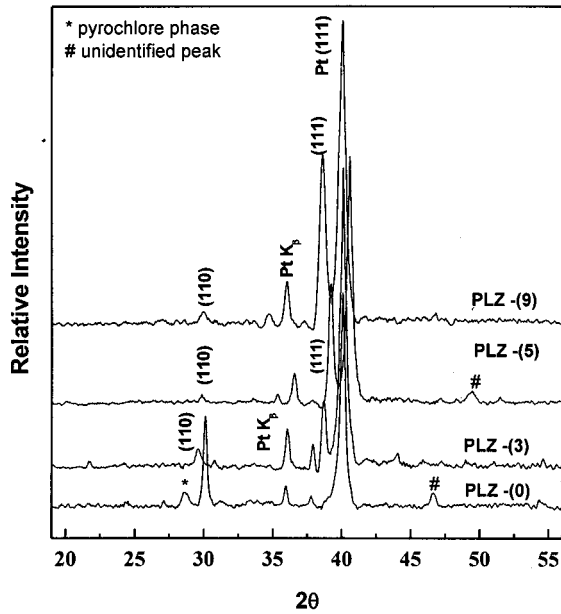


FIG. 1. X-ray-diffraction patterns of (i) PLZ-0, (ii) PLZ-3, (iii) PLZ-5, and (iv) PLZ-9 thin films.

the thin-film processing. Details of the target and the thin-film processing procedure could be found elsewhere.²⁵ Thin films of various La contents in PZ were deposited on Pt-coated Si substrates at a substrate temperature of 550 °C with an oxygen partial pressure of 10–100 mTorr. Physical characterizations, such as x-ray diffraction (Scintag 2000, Cu K_{α} radiation) and energy dispersive x-ray analysis, were employed for the identification of the perovskite phase formation and compositional analysis, respectively. The complex dielectric permittivity and ac electrical properties were measured using an automated Keithley LCZ 3330 meter with an alternating oscillation level of 50 mV over a temperature range of 50–300 °C in a frequency range of 0.1–100 kHz. Polarizations vs applied electric-field hysteresis measurements were done using a ferroelectric test system (Radiant Technologies RT-66A). The x-ray-diffraction patterns of pure and La-modified lead zirconate thin films are shown in Fig. 1. Thin films of PLZ-0 have shown polycrystalline structure, whereas with increase of La content in lead zirconate thin films, the films have shown a high orientation along the pseudocubic (111) direction.

The Raman measurements were performed using an ISA T64000 triple monochromator. An optical microscope with an 80x objective was used to focus the 514.5-nm line of a Coherent Innova 99 Ar⁺ laser on the sample. The same microscope objective collected the backscattered radiation. The scattered light, dispersed by the spectrophotometer, was detected by a charge-coupled device detection system. The spectral resolution of the Raman system was less than 1 cm^{-1} . A microscope compatible heater from Leitz Welzlar was used for temperature-dependent Raman measurements in the range 24–400 °C.

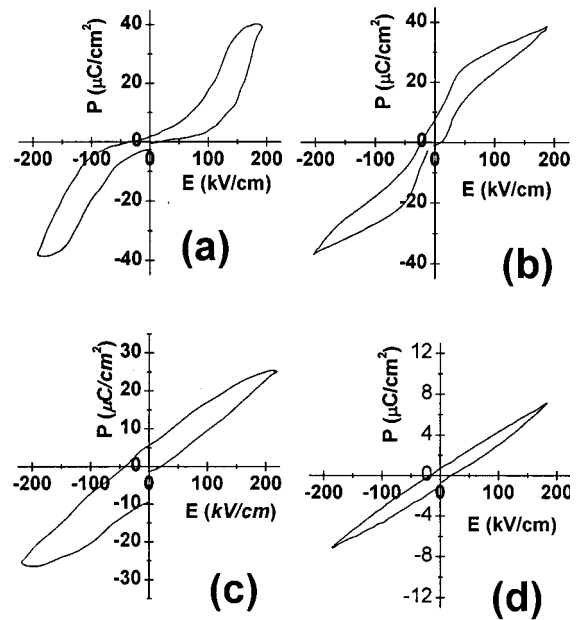


FIG. 2. Polarization hysteresis measurements in the thin films of (a) PLZ-0, (b) PLZ-3, (c) PLZ-5, and (d) PLZ-9.

III. RESULTS AND DISCUSSION

Dielectric and polarization hysteresis properties

Lead zirconate is a room-temperature antiferroelectric composition with the phase-transition temperature of ~ 232 °C.⁶ The role of La^{3+} substitution in PZ thin films has shown significant change in the polarization hysteresis and phase transformation characteristics. The P - E hysteresis measurements are shown in Fig. 2 for PLZ-0, PLZ-3, PLZ-5, and PLZ-9, respectively. The presence of double hysteresis in pure PZ (PLZ-0) confirmed the field-induced antiferroelectric phase transition. The gradual vanishing of double hysteresis behavior followed by a ferroelectric single hysteresis loop and reduction of the maximum polarization with La^{3+} substitution in PZ suggests that domain switching has become easier with the same electric-field strength. On doping with La the majority of the aliovalent La ions are known to go onto the “A” sites, replacing Pb cations.^{26,27} The addition of La to lead zirconate reduced the dielectric phase-transition temperature, changing it from a ferroelectric phase to a paraelectric phase as shown in Fig. 3. The transition temperature shifted towards lower temperature with increasing La^{3+} concentration, and for PLZ-9 thin films, the dielectric phase transition is found at almost room temperature. However, on increasing the La^{3+} content in the films, the height of the dielectric maximum decreased gradually. Shifting the transition temperature towards a lower value with the addition of La to pure PZ thin films can be attributed to softening of the ferroelectric phase, i.e., the orthorhombic antiferroelectric phase to a cubic paraelectric phase through a tetragonal ferroelectric phase. According to lattice dynamics by Cowley, the dielectric properties and phase transitions in PZ are governed by four modes,²⁸ i.e., antiferroelectric modes Σ_3 with vectors $\mathbf{q}(\frac{1}{2}, \frac{1}{2}, 0)\pi/a$ and $M_5' \mathbf{q}(1, 1, 0)\pi/a$,

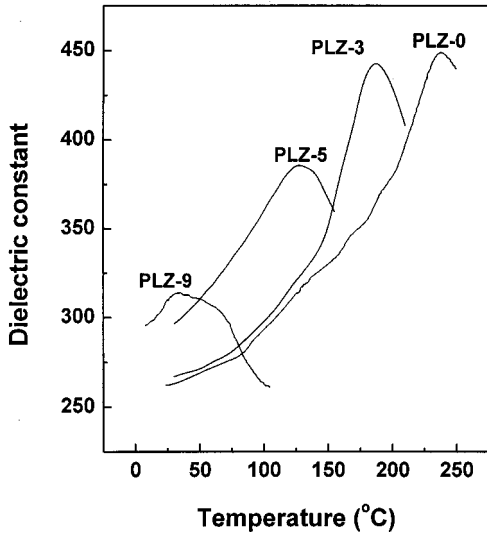


FIG. 3. Dielectric phase transition in La-modified lead zirconate thin films. (i) PLZ-0, (ii) PLZ-3, (iii) PLZ-5, and (iv) PLZ-9, respectively.

a ferroelectric mode Γ_{15} with a vector at the center of Brillouin zone $\mathbf{q}(0,0,0)\pi/a$, and a Γ_{25} with $\mathbf{q}(1,1,1)\pi/a$ at the R corner of the Brillouin zone. Out of these, the major antiferroelectric and ferroelectric modes are Σ_3 and Γ_{15} , and the respective mode equations are

$$\omega_F^2(q=0) = K(T - T_O), \quad (1)$$

$$\omega_A^2(q \neq 0) = K'(T - T_A), \quad (2)$$

where T_A is the transition temperature to the antiferroelectric phase and T_O is the Curie-Weiss temperature.

The antiferroelectric mode Σ_3 is controlled by all the atomic displacements in specific directions, whereas the ferroelectric phase is governed by the displacements of the oxygen atoms in the direction of the c axis. Thus, placing aliovalent atoms in PZ (such as La on the Pb site, in the present case) leads to formation of defects, which will further influence the vibrational frequencies of both the ferroelectric and the antiferroelectric modes, particularly with the influence of oxygen vacancies. Dai, Xu, and Viehland²⁹ observed an earlier hardening of the ferroelectric (FE)²⁹ mode with La-modified lead zirconate ceramics with the chemical formula $\text{Pb}_{1-x}\text{La}_x\text{Zr}_{1-x/4}\text{O}_3$, i.e., under stoichiometric conditions. On the other hand Pb and O vacancies have an opposite effect on the vibrational frequency of the FE mode, i.e., they cause a “hardening” of Γ_{15} , leading to a lowering of paraelectric to ferroelectric phase-transition temperatures. In the present case with the chemical composition of $\text{Pb}_{1-1.5x}\text{La}_x\text{ZrO}_3$, the controlled formation of Pb and O vacancies also causes changes in the vibrational frequency of the AFE mode Σ_3 . From the present set of analyses, the antiferroelectric mode Σ_3 is “hardening,” which favors lowering of the antiferroelectric to ferroelectric phase-transition temperature. Hence, it can be asserted that samples with dif-

ferent microscopic heterogeneities in Pb and O vacancies will definitely decide the divergence of various macroscopic properties.

Ferroelectricity results from condensing a transverse optical-phonon mode at the center of the Brillouin zone, resulting from long-range Coulombic interactions between atomic dipole moments, whereas antiferroelectricity results from condensing a transverse optical phonon at the boundary of the Brillouin zone, resulting from nearest-neighbor interactions between dipole moments. La modification of PZ may not have an intrinsic effect of stabilizing the antiferroelectric state. Rather it might enhance the competition between the short- and long-range dipolar interactions. From the present set of results it is clear that the addition of La^{3+} introduces the lattice defects, such as cation and anion vacancies, reducing the size of the cell volume, and it might suppress antiferroelectricity *via* reducing shorter-range coulombic interactions. Earlier, Dai, Xu, and Viehland²⁹ have explained that La “impurities” could induce competing antiferroelectric and ferroelectric ordering due to the disruption of long-range dipolar interactions. Because of this, the components of spontaneous polarization on the a - b plane may align antiparallel due to strong short-range antiferroelectric couplings and along the c axis perpendicular to the a - b plane.^{30,31} The spontaneous polarization by a ferroelectric mode exists, and is not significantly affected by the AFE couplings in the a - b plane. Very recent studies on barium-modified lead zirconate ceramics have shown a reduction of T_c with an increase of the Ba content.³² These dielectric phase-transition studies are found concurrent with the reduction of tetragonality with an increase in the La content.

Raman spectroscopy results of these films favor the bulk nature of the phenomena involved in the dielectric phase transition. Raman-scattering results show that the La dopant influences strongly the lattice dynamics. At room temperature PbZrO_3 (PZ) has an orthorhombic structure belonging to the space group D_{2h}^9 .³³ Raman spectra from single-crystal PZ have shown certain external modes in the low-frequency region ($\nu < 100 \text{ cm}^{-1}$) related to Pb lattice modes.³⁴ The temperature-dependent Raman spectra of PLZ-0 films are shown in Fig. 4.

A sharp mode at about 136 cm^{-1} softens noticeably with increasing temperature. The decreasing mode intensity with increasing temperature in the pure lead zirconate thin films reflects a phase transition. This mode has been associated with the antiferroelectric (orthorhombic) to ferroelectric (rhombohedral) phase transition at 234°C in PZ single crystals³⁵ and $\text{PbZr}_{0.95}\text{Ti}_{0.05}\text{O}_3$ ceramics.³⁶ The low-frequency ($\nu < 100 \text{ cm}^{-1}$) PZ modes are very sensitive to the temperature and reflect a ferroelectric rhombohedral to paraelectric cubic phase at about 245°C in bulk material.^{35,36} These modes were not resolved in Raman spectra of the present set of La-modified PZ films due to the quasielastic scattering. The changes near the rhombohedral to cubic phase-transition temperature, therefore, are not distinct in the film spectra. Kojima and Dong³⁶ explained the presence of high-frequency Raman modes (above the transition temperature) of $\text{PbZr}_{0.95}\text{Ti}_{0.05}\text{O}_3$ ceramics in terms of defects and local distortions near the grain boundaries. The micro-Raman

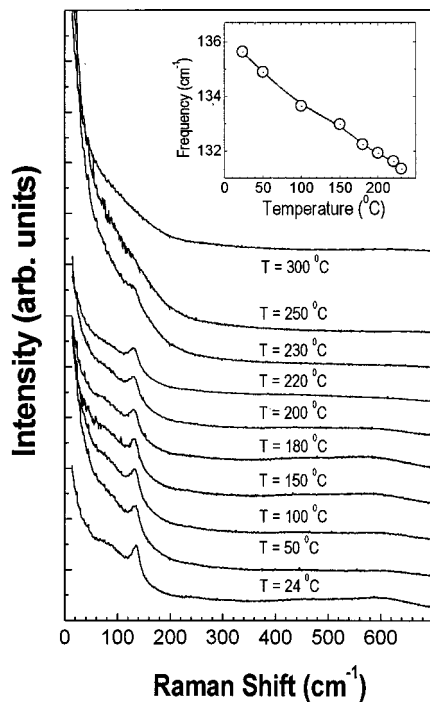


FIG. 4. Micro-Raman spectra of pure PZ (i.e., PLZ-0) at various ambient temperatures.

results therefore, confirm the intermediate ferroelectric phase as observed from polarization measurements in these films. No high-frequency Raman band was detected above 250 cm^{-1} in our films, which indicates a microlevel homogeneity of the material. The temperature-dependent micro-Raman results, therefore, confirm the intermediate ferroelectric phase as observed from polarization measurements. In the high-frequency region, internal modes related to certain polyatomic groups of the material appeared in the spectra. Based on single-crystal work, the bands at 204 and 232 cm^{-1} have been associated with Zr-O bonding, the bands at 285, 330, and 344 cm^{-1} have been assigned to ZrO_3 torsions, and those at 501 and 532 cm^{-1} are due to the Zr-O stretching.³⁷ Figure 5 shows the room-temperature Raman spectra of the present set of La-modified PZ films. The low-frequency modes that have been observed in the Raman spectra of bulk

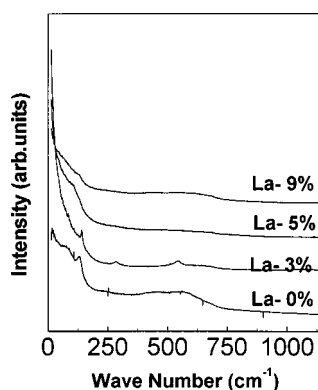


FIG. 5. Micro-Raman spectra of La-modified PZ thin films at room temperature.

material were not observed in these films. Additionally, weak and broad bands appear in the high-frequency region. This is due to the lower scattering volume and film substrate interactions in the present films. The investigation of these phases' coexistence by Raman-scattering measurements indicated that the transition temperatures decreases as the lanthanum content increases, indicating that the character of the transitions becomes more diffuse with increasing lanthanum concentrations. Earlier, coexistence of antiferroelectric, ferroelectric, and paraelectric phases in La-modified PZT bulk ceramics was reported by Pasto and Condrate.³⁷ The existence of two phase transitions and the intermediate ferroelectric phase between the antiferroelectric and paraelectric phases in PZ have been evidenced from x-ray-diffraction and neutron-scattering investigations.^{38,39} Light scattering in single-crystal PZ was studied in the vicinity of the intermediate phase.³⁷ However, no such information of phase transitions exists for thin films of PZ and La-modified PZ thin films. Thus, from the dielectric, hysteresis, and micro-Raman studies it is clear that the addition of La to orthorhombic PLZ-0 thin films transforms from a tetragonal to cubic structure (with 9 mole % of La) gradually.

ac electrical properties

The variation of the ac conductivity with frequency at different temperatures is shown in Fig. 6. The conductivity has increased monotonically with frequency in the measured frequency range from 0.1–100 kHz. A feature common to ac conductivity is a frequency-dependent conductivity that increases approximately linearly with frequency as

$$\sigma(\omega) = A \omega^S \quad (0 < S < 1). \quad (3)$$

It has been observed that the parameter “ S ” in the frequency dependence of conductivity is related to doping and stoichiometry of thin films. The exponent “ S ” is estimated as the slope of $\log \sigma(\omega)$ vs $\log \omega$ and it is found that “ S ” increases with decreasing temperature as shown in Fig. 7. It may be noted that the varied nature of the parameter “ S ” with different mole % of La concentrations in PZ thin films indicates either a broad distribution of relaxation times⁴⁰ or multiple site polaronic hopping.⁴¹ Values of “ S ” less than unity are associated with charge carriers or with “extrinsic” dipoles arising from the presence of defects or impurities. The values of “ S ” have shown a decreasing trend with rising temperature, indicating the interaction between the different charged species decreases as the lattice scales down. The overall trend of ac conductivity characteristics with frequency in Fig. 6 represents a “universal” power law [Eq. (3)], which is based on rigorous many-body dielectric interactions.⁴² Results of ac measurements have begun to appear relating to all manner of materials, and the type of frequency dependence given by the above equation virtually became the hallmark of hopping conduction.¹⁸ The difference in the macroscopic properties between films mainly originates from the difference in the microscopic nature of the charge carriers in each film. It mainly comes from the outermost free-charge carriers and/or trapped charge carriers. The similarity of the response corresponding to very different La concentrations could be

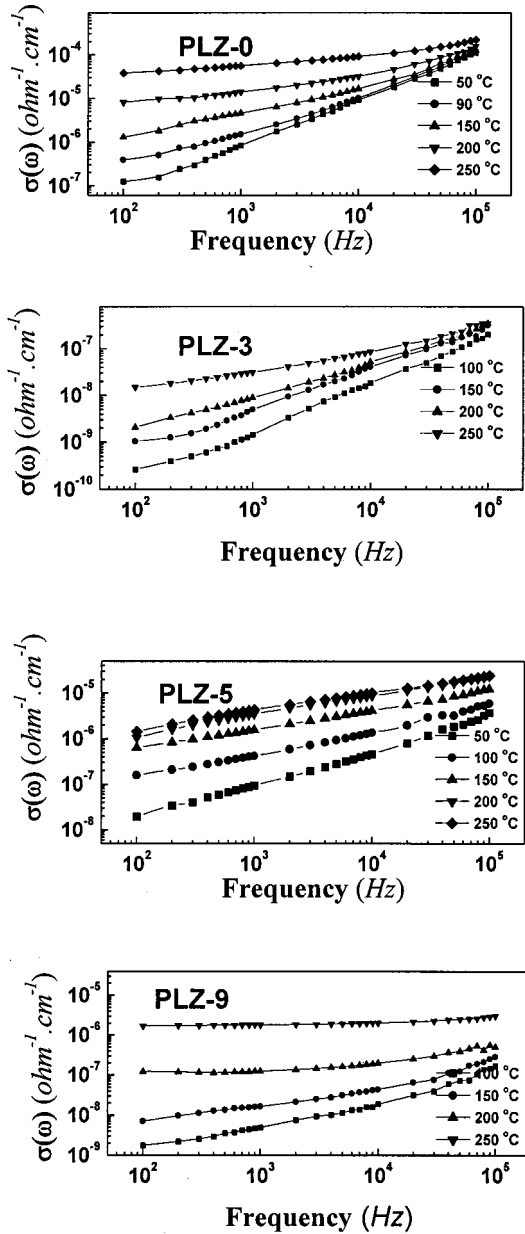


FIG. 6. ac conductivity vs frequency response in La-modified lead zirconate thin films.

due to the interactions among many bodies, such as charged species, regardless of whether they are electrons, ions, dipoles, or defects. In hopping conduction, localized charge carriers at each atomic site jump to another site by thermal energy from time to time. In this case, each jump of a charge carrier is considered to occur completely at random, without any correlation between one jump and the next. An electric field, however, affects the probability of jumps such that carriers move on average, along the field.⁴¹ Arrhenius plots of total conductivity vs $1000/T$ for different La contents of PLZ thin films are shown in Fig. 8. It can be seen that the respective dc activation energies for 3 mole % La-contained films have shown the highest activation energy over all other compositions that have been considered here.

At lower frequencies the ac conductivity is considerably

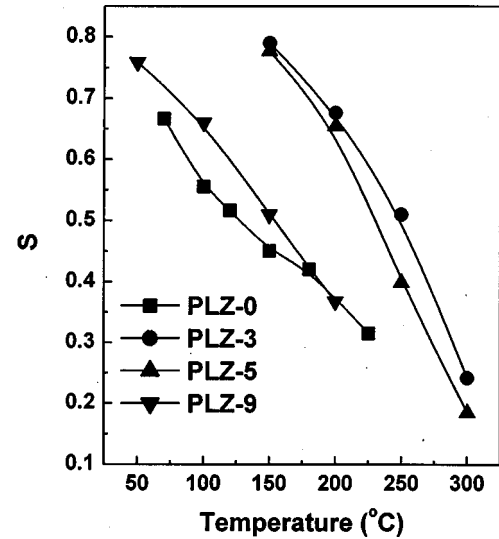


FIG. 7. Variation of exponent “S” with temperature at 100 kHz in La-modified lead zirconate thin films.

higher than the dc conductivity and increases with increasing carriers within the impurity band between occupied and unoccupied donor sites. The ac conductivity of the thin films can arise from both bound as well as free-charge carriers. For instance, if free carriers in nonlocalized states carry the current, the conductivity at frequency ω is given by⁴³

$$\sigma(\omega) = \sigma_{dc} \frac{1}{1 + \omega^2 \tau^2}, \quad (4)$$

where τ is the relaxation time. According to the above expression [Eq. (4)], the frequency response of free carriers diminishes with a rise in frequency ω . In the present context, the increase of ac conductivity indicates that the charge transportation must be related to the hopping of bound carriers trapped in the sample. Such bound charge carriers on the different lattices can be considered as polarons.⁴⁴ Two major physical models have been developed to account for sublinear frequency-dependent conductivity:

(i) In quantum-mechanical tunneling (QMT),⁴¹ a phonon-assisted tunneling of charge carriers between spatially localized states occurs. The energy difference between states will be supplied by the phonon and for purposes of discussion one can view this process as tunneling through the potential barrier separating the localized states. Following the QMT for charge transport the S and absolute temperature are related to

$$\frac{dS}{dT} = \frac{4W_P}{2KT^2} \frac{1}{\left\{ \ln\left(\frac{\nu_O}{\omega}\right) - \left(\frac{W_P}{2KT}\right) \right\}^2}. \quad (5)$$

Equation (5) predicts an increase of S with increasing temperature. However, in the present case, as well as in earlier studies, a decrease of S with increasing temperature was observed.⁴⁵ Attempts to use the QMT model have given a value of S that is closer to 0.8 and suggests an unreasonably high value of phonon frequency, 10^{39} Hz, with a measuring

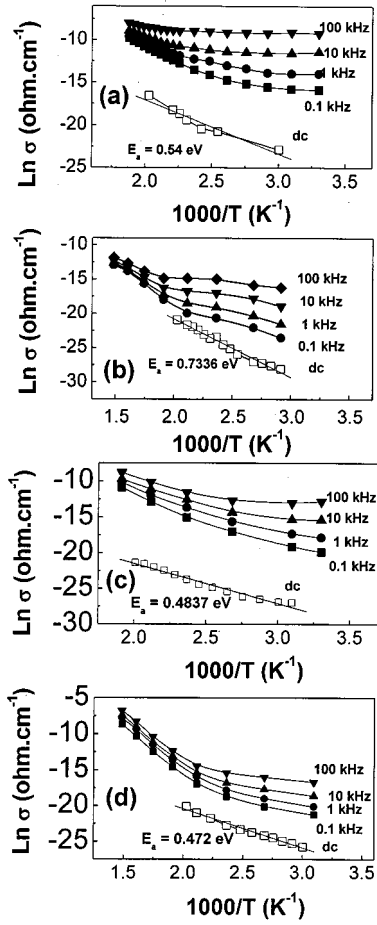


FIG. 8. Arrhenius plots of ac and dc conductivity measurements. (i) PLZ-0, (ii) PLZ-3, (iii) PLZ-5, and (iv) PLZ-9 thin films, respectively.

frequency of 10^5 Hz. Thus, the single phonon-assisted hopping theory of Pollak and Gebelle⁴¹ explains quite well the ac conductivity observed in slightly compensated doped crystalline semiconductors. One must conclude that the extension of this theory to cover materials such as oxide thin films is inadequate.

(ii) In the correlated barrier hopping conduction model⁴⁶ the ac conductivity and charge carriers in which the charge transport between localized states mainly occur due to hopping over the potential barrier separating the sites. The many-body interactions between carriers postulate the correlation in terms of a very low probability of two sites occupied simultaneously, and may be accounted for by Coulombic repulsion with polaron binding energy W_M . The basic assumption is charge transfer by thermal activation over the barrier between two sites, each having a coulombic wells overlap, resulting in a lowering of the effective barrier W_M to the value W , which for the case of a single charge transition is given by

$$W_M - W = \frac{4e^2}{\pi\epsilon_0\epsilon R}. \quad (6)$$

Assuming the defect centers are distributed randomly in space, the activation energy and hopping distances are esti-

mated from the frequency exponent “ S ” as

$$S = 1 - \frac{6kT}{W_M - kT \ln\left(\frac{1}{\omega\tau_0}\right)}, \quad (7)$$

and

$$R_\omega = \frac{e^2}{\pi\epsilon_0\epsilon \left[W_M - kT \ln\left(\frac{1}{\omega\tau_0}\right) \right]}, \quad (8)$$

where τ_0 is the characteristic relaxation time that is in the order of atomic vibrations with periodicity of $\sim 10^{13}$ Hz. The parameter W_M appearing in Eq. (6) is the maximum energy required for the hopping of charge species. From the above expressions it is clear that “ S ” is predicted to be both frequency and temperature dependent, and it can be seen that, at least for moderate temperature ranges, “ S ” increases with increasing frequency and decreases with temperature. For $W_M \gg kT$ the lowest bound to the hopping distance R_ω is

$$R_\omega = \frac{4e^2}{\pi\epsilon_0\epsilon W_M}, \quad (9)$$

and

$$1 - S = \frac{6kT}{W_M}. \quad (10)$$

The lower bound value R_{\min} (cutoff) to the hopping distance R_ω is given by

$$R_{\min} = \frac{2e^2}{\pi\epsilon_0\epsilon W_M}, \quad (11)$$

which is necessary to preclude unphysical negative values of the hopping energy W_M . Using the experimental “ S ” values at 100 kHz and using Eq. (3) the values of W_M were estimated as a function of temperature using Eq. (10) as shown in Fig. 9.

Figure 10 shows the temperature dependence of R_{\min} [estimated from Eq. (11)] of various La^{3+} -concentrated PZ thin films. The activation energy showed a maximum with a minimum of corresponding R_{\min} for PLZ-3 thin films, which indicates once again the correlation between the activation energy and the cutoff hopping distance; i.e., the higher the polaronic coupling with the lattice, the lower the hopping distance. Pramanik, Butchier, and Cox⁴⁷ showed that by using extended pair approximation and percolation conditions the critical percolation radius (R_p) in three dimensions is given by

$$R_p = \left(2.7 \times \frac{3}{4\pi N} \right)^{1/3}. \quad (12)$$

The corresponding activation energy for the dc conductivity $W(R_p)$ is simply the averaged value of the small barrier heights separated by the critical percolation radius R_p :

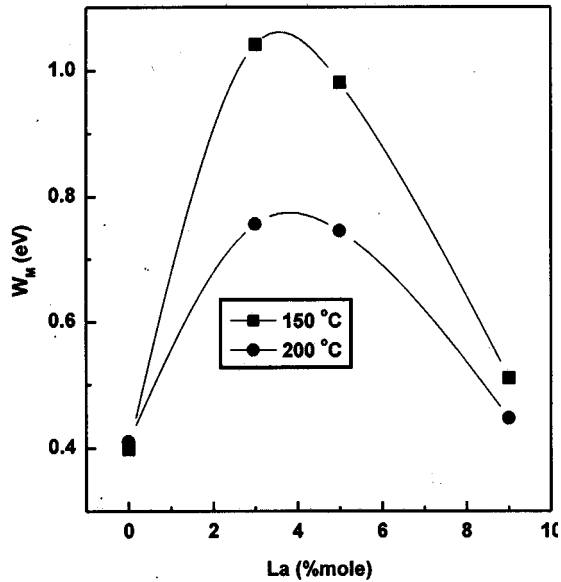


FIG. 9. Hopping energy as a function of La content in PbZrO_3 thin films.

$$W(R_P) = W_M - \frac{2e^2}{\pi \epsilon \epsilon_0 R_P}, \quad (13)$$

where N is the defect concentration in the PLZ films with different concentrations of La content. For the present case the value of N has been considered to be $\sim 10^{19}/\text{cc}$, from our earlier studies on dc electrical properties of these films.⁴⁸

The variation of $W(R_P)$ and R_P is shown in Fig. 11 and the difference in R_P and R_{\min} clearly proves that the ac and dc conductivities in La-modified antiferroelectric PZ thin films are not due to the same mechanisms. This suggests that the ac conduction mechanism is mainly determined by the presence of defect concentration, and coupling between the neighboring polarons. Analysis of dc and ac conductivity using the aforementioned set of expressions suggests that dc

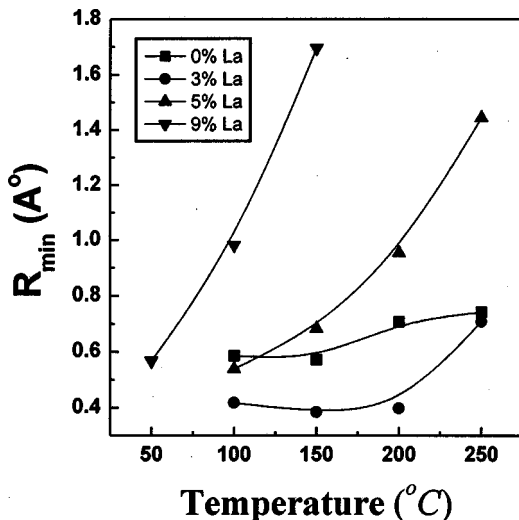


FIG. 10. Minimum hopping distance as a function of temperature in La-modified PbZrO_3 thin films.

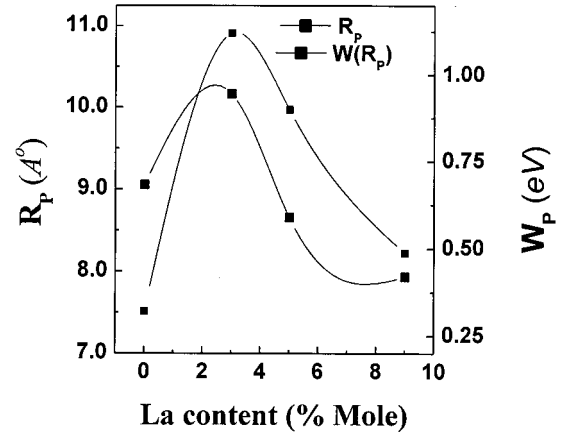
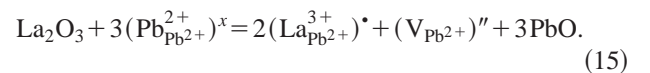
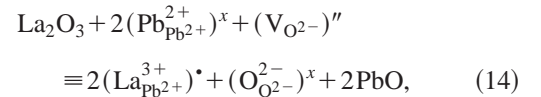


FIG. 11. The variation of $W(R_P)$ and R_P as a function of La content in PbZrO_3 thin films.

conduction requires migration between the long-range potential wells while ac conduction particularly at low temperatures can occur through carrier motion over a shorter range, that being a power law of frequency.⁴⁹ This suggests that though the trap site energy is constant, the hopping energy is mainly determined by the La content in the films, which means that defect chemistry plays a major role in these films.

Adopting Kröger-Vinks notation for the defect chemistry of ionic defects, when oxygen is absorbed into the lattice during processing of films, two holes will be generated. The addition of La_2O_3 to PZ affects the volatility of PbO from the films and increases with increasing La doping. The La_2O_3 doping effect can be considered in Pb-based thin films between the two cases (i) and (ii) as follows:^{50,51}



In the former case, the oxygen vacancies will be reduced with La occupation on the Pb site, leading to a decrease in p -type concentration there by improving the resistivity of the material. For higher La^{3+} concentration, two La ions would replace three Pb ions creating a doubly negatively charged vacant Pb site. In this case, a greater number of holes can be trapped and excess charge carrier on $(\text{La}_{\text{Pb}^{2+}}^{3+})^*$ can participate in conduction or it can form a complex with an ionized Pb vacancy. In reality, both the defect schemes show their influence due to localized evaporation of PbO from the Pb-based thin films during processing. Thus, for larger La doping, elimination of PbO content is more pronounced, and hence, a lower level La^{3+} substitution might lead to compensation of oxygen vacancies initially up to a certain concentration and could enhance the resistivity of the films.^{15,52} A further increase in the La^{3+} content could increase the contribution of charge traps from cationic vacancies. Thus, a gradual increase followed by a fall of activation energy beyond 3 mole % of the addition of La could be visualized in

terms of strong polaronic coupling between the charged carriers and the charge defects, i.e., they suffer an appreciable charge-carrier-lattice (phonon) interaction. Similar is the case of the reduction of the hopping distance up to 3 mole % of the addition of La^{3+} , and beyond $x > 3\%$, the weak polaronic energies might be responsible for an increase in hopping distances in La-modified lead zirconate thin films. The improvement in controlling the leakage current with incorporation of 3 mole % of La^{3+} in PZ thin films from the present analysis is consistent with our earlier dc electrical studies of La^{3+} -modified lead zirconate thin films and some other Pb-based ferroelectric thin films.^{15,25}

IV. CONCLUSIONS

Dielectric and ac electrical properties of antiferroelectric lead zirconate thin films and La-modified lead zirconate thin films have been studied. Doping with La to lead zirconate might weaken the short-range columbic antipolar attractions and thereby improves ferroelectricity followed by paraelec-

tric phases. ac electrical characterizations on La-modified lead zirconate thin films have shown that a polaronic related charge-hopping mechanism is responsible for charge-carrier transportation in these films. Hopping and dc activation energies are found to be maximum for films with 3% La, with a minimum hopping distance. Such a behavior could be attributed to either the formation of defect complexes or some sort of charge-carrier compensation phenomenon at a microscopic level of the films.

ACKNOWLEDGMENTS

The authors would like to acknowledge the financial support from the Indian Space Research Organization and the Department of Science and Technology, India to carry out the present work. One of the authors (S.S.N.B) also acknowledges Professor T.R.N Kutty, Materials Research Center, IISc, for necessary helpful discussions. One of the authors (P.V.) wishes to acknowledge CSIR, India for financial support.

*Present address: EPFL, Lausanne, Switzerland. Email address: srowthi.bharadwaja@epfl.ch

†Author to whom correspondence should be addressed. Email address: sbk@mrc.iisc.ernet.in

¹J. F. Scott and Paz de Aranjo, *Science* **246**, 1400 (1989).

²R. Watton and M. A. Todd, *Ferroelectrics* **118**, 279 (1991).

³Y. Nemirovsky, A. Nemirovsky, P. Murali, and N. Setter, *Sens. Actuators A* **56**, 239 (1996).

⁴D. L. Polla, *Microelectron. Eng.* **29**, 51 (1995).

⁵C. E. Land, P. D. Thacher, and G. H. Haertling, *Appl. Solid State Sci.* **4**, 137 (1974).

⁶F. Jona, G. Shirane, F. Mazzi, and R. Pempinsky, *Phys. Rev.* **105**, 849 (1957).

⁷S. S. N. Bharadwaja and S. B. Krupanidhi, *J. Appl. Phys.* (to be published).

⁸B. Xu, Y. Ye, Q. M. Wand, and L. E. Cross, *J. Appl. Phys.* **85**, 3753 (1999).

⁹T. Tani, J.-F. Li, Dwight Viehland, and D. A. Payne, *J. Appl. Phys.* **75**, 3017 (1994).

¹⁰C. J. Gaskey, K. R. Udayakumar, H. D. Chen, and L. E. Cross, *J. Mater. Res.* **10**, 2764 (1995).

¹¹Long Wu, Tien-Shou Wu, Chung-Chuang Wei, and His-Chuan Liu, *J. Phys. C* **16**, 2823 (1983).

¹²Long Wu, Chung-Chuang Wei, Tien-Shou Wu, and Chain-Cheau Teng, *J. Phys. C* **16**, 2803 (1983).

¹³Duane Dimos, Robert W. Schwartz, and Steven J. Lockwood, *J. Am. Ceram. Soc.* **77**, 3000 (1997).

¹⁴Radosveta D. Klissurska, Alexander K. Tagantsev, Keith G. Brooks, and Nava Setter, *J. Am. Ceram. Soc.* **80**, 336 (1997).

¹⁵C. Sudhama, J. Kim, J. Lee, V. Chikarmane, W. Shepherd, and E. R. Myers, *J. Vac. Sci. Technol. B* **11**, 1302 (1993).

¹⁶Qi Tan, Z. Xu, Jie-Fang Li, and Dwight Viehland, *J. Appl. Phys.* **80**, 5866 (1996).

¹⁷R. D. Klissurka, K. G. Brooks, I. M. Reaney, C. Pawlaczyk, M. Kosec, and N. Setter, *J. Am. Ceram. Soc.* **78**, 1513 (1995).

¹⁸X. Chen, A. I. Kingon, L. Mantese, O. Auciello, and K. Y. Hsieh, *Integr. Ferroelectr.* **3**, 355 (1993).

¹⁹P. Gerthen, R. Groth, and K. H. Härdlt, *Phys. Status Solidi* **11**, 303 (1965).

²⁰R. E. Koritala, M. T. Lanagan, N. Chen, G. R. Bai, Y. Huang, and S. K. Streiffer, *J. Mater. Res.* **15**, 1962 (2000).

²¹S. S. N. Bharadwaja and S. B. Krupanidhi, *Appl. Phys. Lett.* (to be published)

²²S. Sengupta, D. Roberts, J.-F. Li, M. C. Kim, and D. A. Payne, *J. Appl. Phys.* **78**, 1171 (1995).

²³Baomin Xu, Yaohong Ye, and L. E. Cross, *J. Appl. Phys.* **87**, 2507 (2000).

²⁴K. Yamakawa, S. Trolier-McKinstry, J. P. Dougherty, and S. B. Krupanidhi, *Appl. Phys. Lett.* **67**, 2014 (1995).

²⁵S. S. N. Bharadwaja and S. B. Krupanidhi (unpublished).

²⁶K. H. Hardtl and D. Henning, *J. Am. Ceram. Soc.* **55**, 230 (1972).

²⁷Masao Takahashi, *Jpn. J. Appl. Phys.* **9**, 1236 (1970).

²⁸M. E. Lines and A. M. Glass, *Principles and Applications of Ferroelectrics and Related Materials* (Clarendon, Oxford, 1977).

²⁹X. Dai, Z. Xu, and D. Viehland, *J. Appl. Phys.* **77**, 5086 (1995).

³⁰Xunhu Dai, Jie-Fang Li, and Dwight Viehland, *Phys. Rev. B* **51**, 2651 (1995).

³¹M. E. Lines and A. M. Glass, *Principles and Applications of Ferroelectrics and Related Materials* (Ref. 28), Ch. 8.

³²Bhadra P. Pokharel and Dhananjai Pandey, *J. Appl. Phys.* **88**, 5364 (2000).

³³H. Fujishita, Y. Shiozaki, N. Achiwa, and E. Sawaguchi, *J. Phys. Soc. Jpn.* **51**, 3583 (1982).

³⁴C. C. Nedelec, I. E. Harrad, J. Handerek, F. Brehat, and B. Wyncke, *Ferroelectrics* **125**, 483 (1992).

³⁵K. Roleder, G. E. Kugel, J. Handerek, M. D. Fontana, C. Carabatos, M. Hafid, and A. Kania, *Ferroelectrics* **80**, 161 (1988).

³⁶S. Kojima and X. Dong, *Jpn. J. Appl. Phys., Part 1* **37**, 5400 (1998).

³⁷A. E. Pasto and R. E. Condrate, *J. Am. Ceram. Soc.* **56**, 436 (1993).

³⁸C. Cochran and A. Zia, *Phys. Status Solidi* **25**, 273 (1968).

³⁹R. W. Whatmore and A. M. Glazer, *J. Phys. C* **12**, 1505 (1979).

- ⁴⁰A. Mansingh, J. M. Reyes, and M. Sayer, *J. Non-Cryst. Solids* **7**, 12 (1972).
- ⁴¹M. Pollak and T. H. Geballe, *Phys. Rev.* **122**, 1742 (1961).
- ⁴²A. K. Jonscher, in *Dielectric Relaxation in Solids* (Chelsea, New York, 1980).
- ⁴³A. I. Lakatos and M. Abkowitz, *Phys. Rev. B* **3**, 1791 (1971).
- ⁴⁴N. Tsuda, K. Nasu, A. Yanase, and K. Siratori, *Electronic Conduction in Oxides* (Springer-Verlag, London).
- ⁴⁵M. Sayer, A. Mansingh, J. M. Reyes, and G. Rosenblatt, *J. Appl. Phys.* **42**, 2857 (1971).
- ⁴⁶G. E. Pike, *Phys. Rev. B* **6**, 1572 (1972).
- ⁴⁷M. H. A. Pramanik, P. N. Butchier, and I. D. Cox, *Philos. Mag. B* **47**, 437 (1983).
- ⁴⁸S. S. N. Bharadwaja and S. B. Krupanidhi (unpublished).
- ⁴⁹M. Sayer, A. Mansingh, J. B. Webb, and J. Noad, *J. Phys. C* **11**, 315 (1978).
- ⁵⁰M. V. Raymond and D. M. Smyth, *Integr. Ferroelectr.* **4**, 145 (1994).
- ⁵¹Sanjeev Aggarwal and R. Ramesh, *Annu. Rev. Mater. Sci.* **28**, 463 (1998).
- ⁵²Z. Ujima, D. Dmytrów, and M. Pawetczyk, *Ferroelectrics* **120**, 211 (1991).